

Supplementary Information to

C–X vs C–H activation for the synthesis of the cyclometalated complexes [Pd(YPhbpy)X] (HPhbpy = 6-phenyl-2,2'-bipyridine; X/Y = (pseudo)halides)

René von der Stück, Simon Schmitz, Axel Klein,*

* to whom correspondence should be addressed. Email: axel.klein@uni-koeln.de; Internet: <http://www.klein.uni-koeln.de/>

Contents:

1. Syntheses

2. Supplementary Figures

Figure S1. 300 MHz ^1H NMR spectrum of F–Phbpy in CDCl_3 .

Figure S2. 300 MHz ^1H NMR spectra of the protoligands X–Phbpy (X = Cl, Br, I) in CDCl_3 .

Figure S3. 300 MHz ^1H NMR spectrum of Cl–Phbpy in CDCl_3 .

Figure S4. 300 MHz ^1H NMR spectrum of Br–Phbpy in CDCl_3 .

Figure S5. 300 MHz ^1H NMR spectrum of I–Phbpy in CDCl_3 .

Figure S6. 300 MHz ^1H NMR spectrum of HO–Phbpy in CDCl_3 .

Figure S7. 300 MHz ^1H NMR spectrum of MeO–Phbpy in CDCl_3 .

Figure S8. 300 MHz ^1H NMR spectrum of TfO–Phbpy in CDCl_3 .

Figure S9. 282 MHz ^{19}F NMR spectrum of TfO–Phbpy in CDCl_3 .

Figure S10. View on the crystal structure of $[\text{BrPhbpyH}]\text{Cl}\cdot 2\text{H}_2\text{O}$ along the *a* and *b* axes.

Figure S11. Molecular structure of $[\text{BrPhbpyH}]\text{Cl}\cdot 2\text{H}_2\text{O}$ and essential metric data.

Figure S12. UV-vis absorption spectra of FPhbpy, ClPhbpy, BrPhbpy, IPhbpy, HOPhbpy, and HPhbpy in CH_2Cl_2 .

Figure S13. Cyclic voltammograms of FPhbpy (left) and HOPhbpy (right) in 0.1 M *n*-Bu₄NPF₆/THF.

Figure S14. Cyclic voltammograms of ClPhbpy in 0.1 M *n*-Bu₄NPF₆/THF.

Figure S15. 600 MHz ^1H NMR spectra of $[\text{Pd}(\text{FPhbpy})\text{Cl}]$, $[\text{Pd}(\text{ClPhbpy})\text{Cl}]$, $[\text{Pd}(\text{BrPhbpy})\text{Cl}]$, $[\text{Pd}(\text{MeOPhbpy})\text{Cl}]$ and 300 MHz ^1H NMR of $[\text{Pd}(\text{IPhbpy})\text{Cl}]$ in DMSO-*d*₆.

Figure S16. 600 MHz ^1H NMR spectrum of $[\text{Pd}(\text{OHPhbpy})\text{Cl}]$ in DMSO-*d*₆.

Figure S17. 600 MHz ^1H NMR spectrum of $[\text{Pd}(\text{TfOPhbpy})\text{Cl}]$ in DMSO-*d*₆.

Figure S18. View on the crystal structure of $[\text{Pd}(\text{MeOPhbpy})\text{Cl}]$ along the crystallographic *b* axis and selected π stacking and Pd···Pd contacts.

Figure S19. Cyclic voltammograms of $[\text{Pd}(\text{ClPhbpy})\text{Cl}]$ and $[\text{Pd}(\text{BrPhbpy})\text{Cl}]$ in 0.1 M *n*-Bu₄NPF₆/THF.

Figure S20. Cyclic voltammograms of $[\text{Pd}(\text{MeOPhbpy})\text{Cl}]$ and $[\text{Pd}(\text{Phbpy})\text{Cl}]$ in 0.1 M *n*-Bu₄NPF₆/THF.

Figure S21. UV-vis absorption spectra of ClPhbpy, $[\text{Pd}_2(\text{dba})_3]$, and $[\text{Pd}(\text{Phbpy})\text{Cl}]$ in THF.

Figure S22. UV-vis absorption spectra of $[\text{Pd}(\text{Phbpy})\text{I}]$ during electrochemical reduction and re-oxidation in 0.1 M *n*-Bu₄NPF₆/THF.

3. Supplementary Tables

Table S1. UV-vis absorption maxima of the protoligands XPhbpy.

Table S2. Parameters of crystal structure solution and refinement for $[\text{Pd}(\text{MeOPhbpy})\text{Cl}]$ and $[\text{Pd}(\text{FPhbpy})\text{Cl}]$.

Table S3. Selected structural parameters of $[\text{Pd}(\text{MeOPhbpy})\text{Cl}]$ and $[\text{Pd}(\text{FPhbpy})\text{Cl}]$.

Table S4. UV-vis absorption maxima Pd complexes $[\text{Pd}(\text{XPhbpy})\text{X}]$.

Table S5. DFT-calculated long-wavelength singlet transitions and UV-vis absorption maxima of $[\text{Pd}(\text{Phbpy})\text{Cl}]$.

Table S6. DFT-calculated long-wavelength singlet transitions and UV-vis absorption maxima of $[\text{Pd}(\text{ClPhbpy})\text{Cl}]$.

Table S7. Selected DFT-calculated long-wavelength singlet and triplet transitions and UV-vis absorption maxima of $[\text{Pd}(\text{OHPhbpy})\text{Cl}]$.

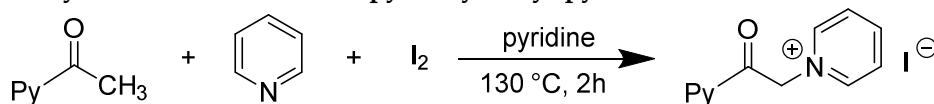
Table S8. DFT-calculated long-wavelength singlet transitions and UV-vis absorption maxima of $[\text{Pd}(\text{MeOPhbpy})\text{Cl}]$.

1. Syntheses

1.1 Synthesis of 2'-iodoacetophenone

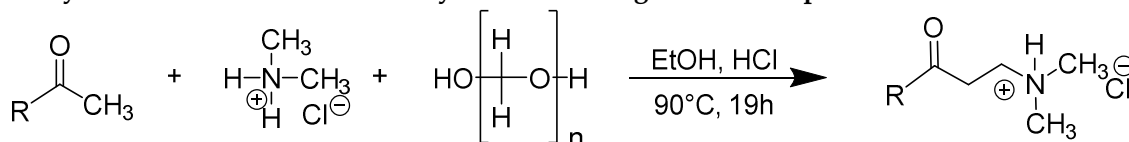
In a 500 mL tree necked round bottom flask 17.26 g (90 mmol) *para*-toluenesulfonic acid monohydrate in 120 mL MeCN have been solved completely. Subsequently 3.65 mL (4.06 g, 30 mmol) 2'-aminoacetophenone were added. A solution of 4.15 g (30 mmol) NaNO₃ and 12.57 (75 mmol) KI in 20 mL H₂O were added dropwise using a dropping funnel while cooling the reaction mixture with crushed ice. The mixture turned dark brown and an intense gas formation was observed. 100 mL of MeCN were added to maintain the stirring. The solution was allowed to warm up to room temperature and was stirred for another 12 h. After addition of 100 mL H₂O, 100 mL 1 M NaHSO₄ solution and 24 mL 2 M Na₂S₂O₃ (thiosulfate) a colour change to bright red was observed. The solution was extracted 3 × with 100 mL portions of ethyl acetate. The united organic phases were washed with 100 mL 1 M HCl, 100 mL 1M NaHSO₄ solution; 50 mL saturated NaCl solution and dried over MgSO₄. Removing the ethyl acetate gave orange oil. Yield: 6.61 g (26.9 mmol, 89.5%) (Lit.: 85%) [1]. ¹H NMR (300 MHz, CDCl₃): δ = 7.93 (dd, 1H, J = 7.9, 0.8 Hz), 7.49-7.37 (m, 2H), 7.12 (ddd, 1H, J = 7.9, 7.2, 1.9 Hz), 2.61 (s, 3H).

1.2 Synthesis of N-1-(2-oxo-2-(pyridinyl)ethyl)pyridinium iodide



In a 250 mL round bottom flask 25.39 g (100 mmol) iodine have been stirred in 100 mL pyridine for ten min until a black solution resulted. Subsequently 11.2 mL (12.1 g, 100 mmol) 2-acetylpyridine was added dropwise. After stirring under reflux for 160 min the reaction mixture was cooled to room temperature. The black precipitate was filtered off using a Büchner funnel, washed with 70 mL of cold pyridine and 50 mL CH₂Cl₂ and dried in vacuum. Yield: 26.34 g (80.8 mmol, 81%). ¹H NMR (300 MHz, DMSO-d₆): δ = 9.03 (d, 2H, J = 6.4 Hz), 8.90-8.86 (m, 1H), 8.74 (t, 1H, J = 7.8 Hz), 8.33-8.24 (t, 2H), 8.18-8.05 (m, 2H), 7.84 (ddd, 1H, J = 7.3, 4.8, 1.5 Hz), 6.52 (s, 2H).

1.3 Synthesis of the Mannich base hydrochlorides – general description



One equivalent of the corresponding acetyl compound, 1.25 eq. dimethylamine hydrochloride and 1.5 eq. paraformaldehyde were suspended in EtOH. After addition of 2 mL concentrated HCl, the reaction mixture was stirred at 90 °C for 19 h. The resulting solution was cooled to ambient temperature and 200 mL of acetone were added. The solution was stored at -26 °C for another 14 h. A colourless, crystalline precipitate was filtered off, washed with acetone and dried under reduced pressure.

1-(phenyl)-3-dimethylaminopropane-1-one-hydrochloride. From 7.21 g (6.99 mL, 60 mmol) acetophenone, 6.12 g (75 mmol) dimethylamine hydrochloride, 2.7 g (90 mmol) paraformaldehyde, 50 mL EtOH. Yield: 8.66 g (41.5 mmol, 68 %) colourless solid. ¹H NMR (300 MHz, CDCl₃): δ = 12.52 (s, 1H), 8.06-7.93 (m, 2H), 7.67-7.55 (m, 1H), 7.54-7.41 (m, 2H), 3.76 (t, J = 6.8 Hz, 2H), 3.55 (t, J = 6.8 Hz, 2H), 2.88 (s, 6H) ppm. ¹³C NMR (75 MHz, CDCl₃): δ = 195.9, 135.5, 134.2, 128.9, 128.3, 52.8, 43.4, 33.9 ppm.

1-(2-fluorophenyl)-3-dimethylaminopropane-1-one-hydrochloride. From 9.26 g (8.14 mL, 67 mmol, 1 eq) 2'-fluoroacetophenone, 6.91 g (72 mmol, 1.3 eq) dimethylamine hydrochloride, 3.02 g (100.5 mmol, 1.5 eq) paraformaldehyde, in 50 mL EtOH. Yield: 7.74 g (33.4 mmol, 50%) colourless material. ¹H NMR (300 MHz, CD₂Cl₂): δ = 12.89 (s, 1H), 7.84-7.79 (t, 1H), 7.56-7.49 (m, 1H), 7.23-7.09 (m, 2H), 3.62-3.53 (t, 2H), 3.41-3.34 (q, 2H), 2.72-2.71 (d, 6H) ppm.

1-(2-chlorophenyl)-3-dimethylaminopropane-1-one-hydrochloride. From 9.27 g (7.8 mL, 60 mmol, 1 eq) 2'-chloroacetophenone, 7.17 g (88 mmol, 1.5 eq) dimethylamine hydrochloride, 2.75 g (90 mmol, 1.5 eq) paraformaldehyde, 50 mL EtOH. Yield 6.28 g (25.3 mmol, 42%) colourless solid. ¹H NMR (300 MHz, DMSO-

d₆): δ = 10.87 (s, 1H), 7.84-7.81 (d, 1H), 7.59-7.58 (d, 2H), 7.55-7.48 (m, 1H), 3.60-3.55 (t, 2H), 3.39-3.37 (t, 2H), 2.78 (s, 6H) ppm.

1-(2-bromophenyl)-3-dimethylaminopropane-1-one-hydrochloride. From 6.83 g (4.6 mL, 34.3 mmol) 2'-bromoacetophenone, 4.93 g (60.46 mmol) dimethylamine hydrochloride and 1.32 g (43.96 mmol) paraformaldehyde, in 30 mL EtOH. Yield: 4.02 g (13.4 mmol, 40%). ¹H NMR (300 MHz, CD₂Cl₂): δ = 12.89 (s, 1H), 7.55 (ddd, 2H, J = 17.2, 7.7, 1.6 Hz), 7.33 (dtd, 2H, J = 17.1, 7.5, 1.5 Hz), 3.59 (t, 2H, J = 7.1 Hz), 3.37 (dd, 2H, J = 12.1, 6.8 Hz), 2.73 (d, 6H, J = 4.8 Hz). ¹H NMR (300 MHz, DMSO-d₆): δ = 10.93 (s, 1H), 7.78 (ddd, J = 12.8 Hz, 2H), 7.61-7.42 (m, 2H), 3.56 (t, 2H), 3.41 (d, J = 7.4 Hz, 2H), 2.78 (s, 6H).

1-(2-iodophenyl)-3-dimethylaminopropane-1-one-hydrochloride. From 6.05 g (24.95 mmol) 2'-iodoacetophenone, 2.51 g (30.74 mmol) dimethylamine hydrochloride, 1.11 g (36.88 mmol) paraformaldehyde, in 20 mL EtOH. Yield: 3.07 g (9.04 mmol, 38%) orange solid. ¹H NMR (300 MHz, DMSO-d₆): δ = 10.88 (s, 1H), 8.02 (dd, 1H, J = 7.9, 0.9 Hz), 7.80 (dd, 1H, J = 7.7, 1.5 Hz), 7.57 (td, 1H, J = 7.6, 1.1 Hz), 7.29 (td, 1H, J = 7.7, 1.6 Hz), 3.59-3.51 (m, 2H), 3.43-3.35 (m, 2H), 2.79 (d, 6H, J = 4.8 Hz).

1-(2-hydroxyphenyl)-3-dimethylaminopropane-1-one-hydrochloride. From 4.06 g (30 mmol) 2'-hydroxyacetophenone, 3.03 g (37.50 mmol) dimethylamine hydrochloride, 1.35 g (45 mmol) paraformaldehyde, in 30 mL EtOH. Yield: 6.12 g (26.6 mmol, 89%) colourless crystals. ¹H NMR (300 MHz, CDCl₃): δ = 12.55 (s, 1H), 11.69 (s, 1H), 7.86 (dd, J = 8.1 Hz, 1H), 7.52 (t, J = 7.0 Hz, 1H), 7.13-6.78 (m, 2H), 3.82 (t, J = 7.0 Hz, 2H), 3.53 (t, J = 7.0 Hz, 2H), 2.90 (s, 6H).

1.4 Synthesis of the Y-C^NN protoligands (Y = F, Cl, Br, I, OH). Kröhnke pyridine synthesis – general description:

One equivalent of the corresponding pyridinium iodide and 12.5 equivalents of ammonium acetate were suspended in glacial acetic acid and stirred for 20 min at 90 °C. Then one equivalent of the Mannich base hydrochloride was added and the reaction mixture was stirred for 20 h at 130 °C. After the removal of the glacial acetic acid, 50 mL of water and 50 mL of CHCl₃ were added, and everything was mixed vigorously. Sometimes a black precipitate was observed. In these cases, it had to be filtered off before continuing. After separation of the two phases, the CHCl₃ phase was washed with 30 mL of H₂O (2×) and 30 mL of brine and subsequently dried over MgSO₄. The solvent was removed under reduced pressure. The crude product (black oil) was either filtered over a small amount of silica or purified via flash chromatography. In some cases, a recrystallisation from EtOH was necessary. The products were dried under reduced pressure.

6-(2-Fluorophenyl)-2,2'-bipyridine (FPhbpy). From 2.24 g (9.67 mmol) 1-(2-fluorophenyl)-3-dimethylaminopropane-1-one-hydrochloride, 3.30 g (10.12 mmol) *N*-1-(2-oxo-2-(pyridinyl)ethyl)pyridinium iodide, 50 mL glacial acetic acid; Yield: 0.92 g (3.7 mmol, 38%) brown solid. ¹H NMR (300 MHz, CDCl₃): δ = 8.70 (ddd, 1H, J = 4.8 Hz), 8.58 (dt, 1H, J = 8.0 Hz), 8.40 (dd, 1H, J = 7.3 Hz), 8.19 (td, 1H, J = 7.8 Hz), 7.93-7.78 (m, 3H), 7.44-7.36 (m, 1H), 7.35-7.27 (m, 2H), 7.18 (ddd, 1H, J = 11.5 Hz).

6-(2-Chlorophenyl)-2,2'-bipyridine (ClPhbpy). From 8.41 g (33.89 mmol) 1-(2-chlorophenyl)-3-dimethylaminopropane-1-one-hydrochloride, 9.80 g (30.05 mmol) *N*-1-(2-oxo-2-(pyridinyl)ethyl)pyridinium iodide, 230 mL glacial acetic acid. Yield: 4.08 g (15.3 mmol, 51%) light brown solid. ¹H NMR (300 MHz, CDCl₃): δ = 8.66 (ddd, J = 4.8, 1.7, 0.9 Hz, 2H), 8.50 (dt, J = 8.0, 1.0 Hz, 2H), 8.41 (dd, J = 7.9, 1.0 Hz, 2H), 7.83 (t, J = 7.8 Hz, 2H), 7.77-7.60 (m, 6H), 7.51-7.43 (m, 2H), 7.38-7.19 (m, 7H). ¹³C NMR (75 MHz, CDCl₃): δ = 156.09 (s), 156.05 (s), 155.82 (s), 149.05 (s), 139.24 (s), 136.80 (s), 136.76 (s), 132.31 (s), 131.80 (s), 130.19 (s), 129.53 (s), 126.93 (s), 124.67 (s), 123.72 (s), 121.35 (s), 119.57 (s).

6-(2-Bromophenyl)-2,2'-bipyridine (BrPhbpy). From 2.38 g (8.03 mmol) 1-(2-bromophenyl)-3-dimethylaminopropane-1-one-hydrochloride, 2.64 g (8.03 mmol) *N*-1-(2-oxo-2-(pyridinyl)ethyl)pyridinium iodide, 50 mL glacial acetic acid. Yield: 1.4 g (4.5 mmol, 56%) brown solid. ¹H NMR (300 MHz, CDCl₃): δ = 8.72 (m, J = 4.8, 1.8, 0.9 Hz, 1H), 8.55 (dt, J = 8.0, 1.1 Hz, 1H), 8.44 (dd, J = 7.9, 1.0 Hz, 1H), 7.92 (t, J = 7.8, 1.4 Hz, 1H), 7.86-7.78 (m, 1H), 7.74 (dd, J = 8.0, 1.0 Hz, 1H), 7.70-7.60 (m, 2H), 7.46 (td, J = 7.5, 1.2 Hz, 1H), 7.36-7.28 (m, 2H) ppm.

6-(2-Iodophenyl)-2,2'-bipyridine (IPhbpy). From 2.95 g (8.69 mmol) 1-(2-iodophenyl)-3-dimethylaminopropane-1-one-hydrochloride, 2.83 g (8.69 mmol) *N*-1-(2-oxo-2-(pyridinyl)ethyl)pyridinium iodide, 75 mL glacial acetic acid. Yield: 1.26 g (3.52 mmol, 41%) brown solid. ¹H NMR: (300 MHz, DMSO-d₆): δ = 8.72 (ddd, 1H, J = 4.8 Hz), 8.50-8.37 (m, 2H), 8.06 (t, 2H, J = 7.8 Hz), 7.95 (m, 1H, J = 7.7 Hz), 7.64-7.52 (m,

3H), 7.47 (m, 1H, $J = 7.5$ Hz), 7.27-7.14 (m, 1H) ppm. $^1\text{H NMR}$ (300 MHz, CDCl_3): $\delta = 8.71$ (dt, $J = 7.5, 2.2$ Hz, 1H), 8.59 (d, $J = 8.0$ Hz, 1H), 8.44 (dt, $J = 7.4, 3.7$ Hz, 1H), 8.03 (dd, $J = 7.9, 0.9$ Hz, 1H), 7.91 (t, $J = 7.8$ Hz, 1H), 7.86-7.77 (m, 1H), 7.54 (ddd, $J = 10.1, 7.7, 1.3$ Hz, 2H), 7.46 (td, $J = 7.5, 1.1$ Hz, 1H), 7.36-7.26 (m, 1H), 7.11 (td, $J = 7.8, 1.8$ Hz, 1H) ppm.

6-(2-hydroxyphenyl)-2,2'-bipyridine (HOPhbp). From 2.75 g (11.97 mmol) 1-(2-hydroxyphenyl)-3-dimethylaminopropane-1-one-hydrochloride, 3.90 g (11.97 mmol) *N*-1-(2-oxo-2-(pyridinyl)ethyl)pyridinium iodide, 100 mL glacial acetic acid. Yield: 1.18 g (4.75 mmol, 40%) brown solid. $^1\text{H NMR}$ (300 MHz, CDCl_3): $\delta = 14.59$ (s, 1H), 8.74 (ddd, 1H, $J = 4.8$ Hz), 8.33 (dd, 1H, $J = 7.0$ Hz), 8.20 (dt, 1H, $J = 7.9$ Hz), 8.05-7.92 (m, 2H), 7.92-7.82 (m, 2H), 7.43-7.30 (m, 2H), 7.07 (dd, 1H, $J = 8.2$ Hz), 6.96 (m, 1H, $J = 8.3$ Hz) ppm.

1.5 Synthesis of 6-(2-methoxyphenyl)-2,2'-bipyridine (MeOPhbp)

Under an argon atmosphere 223.73 mg (0.9 mmol) 6-(2-hydroxyphenyl)-2,2'-bipyridine were dissolved in 17 mL dry THF. During the addition of 151.48 mg (1.35 mmol) *KOt*Bu and 280.14 μL (4.5 mmol) MeI the formation of an orange suspension was observed. After stirring at ambient temperature for 16 h, 75 mL of CH_2Cl_2 were added. The solution was washed 3 \times with 30 mL H_2O and dried over MgSO_4 . After removal of the solvent under reduced pressure, the product was obtained as brown oil. Yield: 130 mg (0.50 mmol, 55%). $^1\text{H NMR}$: (300 MHz, CDCl_3): $\delta = 8.69$ (ddd, 1H, $J = 4.9$ Hz), 8.57 (dt, 1H, $J = 8.0$ Hz), 8.33 (dd, 1H, $J = 7.7$ Hz), 8.01 (dd, 1H, $J = 7.6$ Hz), 7.92 (dd, 1H, $J = 7.9$ Hz), 7.89-7.76 (m, 2H), 7.40 (td, 1H), 7.30 (ddd, 1H, $J = 7.5, 1.2$ Hz), 7.13 (td, 1H, $J = 7.5$ Hz), 7.04 (d, 1H, $J = 8.3$ Hz), 3.90 (s, 3H) ppm.

1.6 Synthesis of 6-(2-triflatophenyl)-2,2'-bipyridine (TfOPhbp)

Under an argon atmosphere 213.80 mg (0.86 mmol) 6-(2-hydroxyphenyl)-2,2'-bipyridine were dissolved in 17 mL dry THF. During the addition of 144.8 mg (1.3 mmol) *KOt*Bu the formation of a dark red solution was observed. The addition of 217.4 mg (1.3 mmol) and stirring for 20 h at ambient temperature led to the formation of a yellow solution. 75 mL water was added. The mixture was extracted 3 \times with 30 mL CH_2Cl_2 . The combined organic layers were dried over MgSO_4 . After removal of the solvent the product was obtained as yellow oil. Yield: 0.33 g (0.86 mmol, 100%). $^1\text{H NMR}$ (300 MHz, CDCl_3): $\delta = 8.77$ (d, 1H, $J = 4.3$ Hz), 8.57 (d, 1H, $J = 8.0$ Hz), 8.49 (dd, 1H, $J = 7.9$ Hz), 8.00-7.84 (m, 3H), 7.65 (dd, 1H, $J = 7.8$ Hz), 7.52 (ddd, 2H, $J = 7.4$ Hz), 7.47-7.33 (m, 2H). $^{19}\text{F NMR}$: (282 MHz, CDCl_3) $\delta = -73.9$.

Supplementary Figures

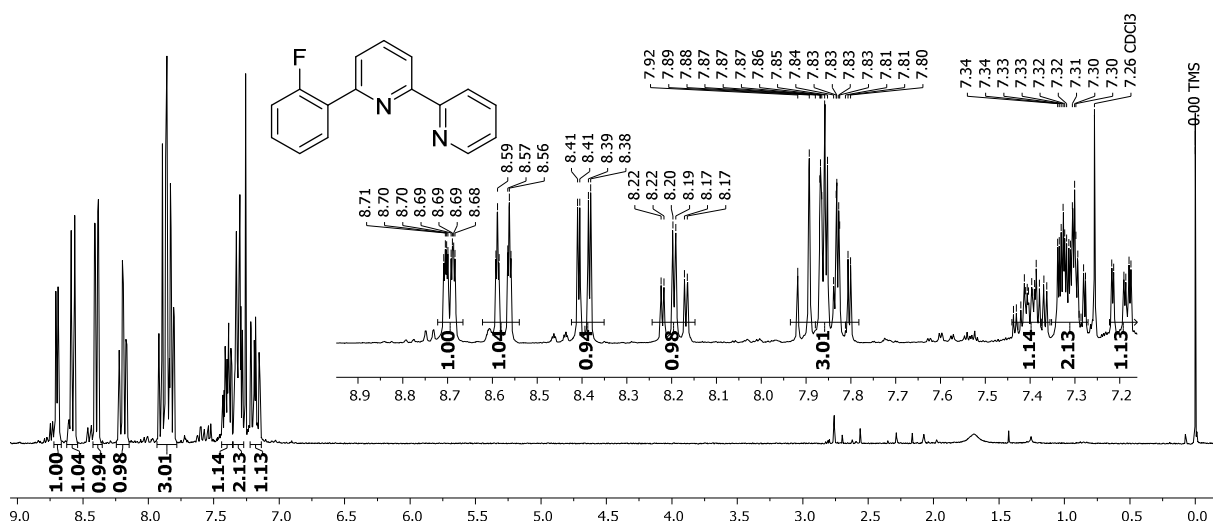


Figure S1. 300 MHz $^1\text{H NMR}$ spectrum of F-Phbp in CDCl_3 .

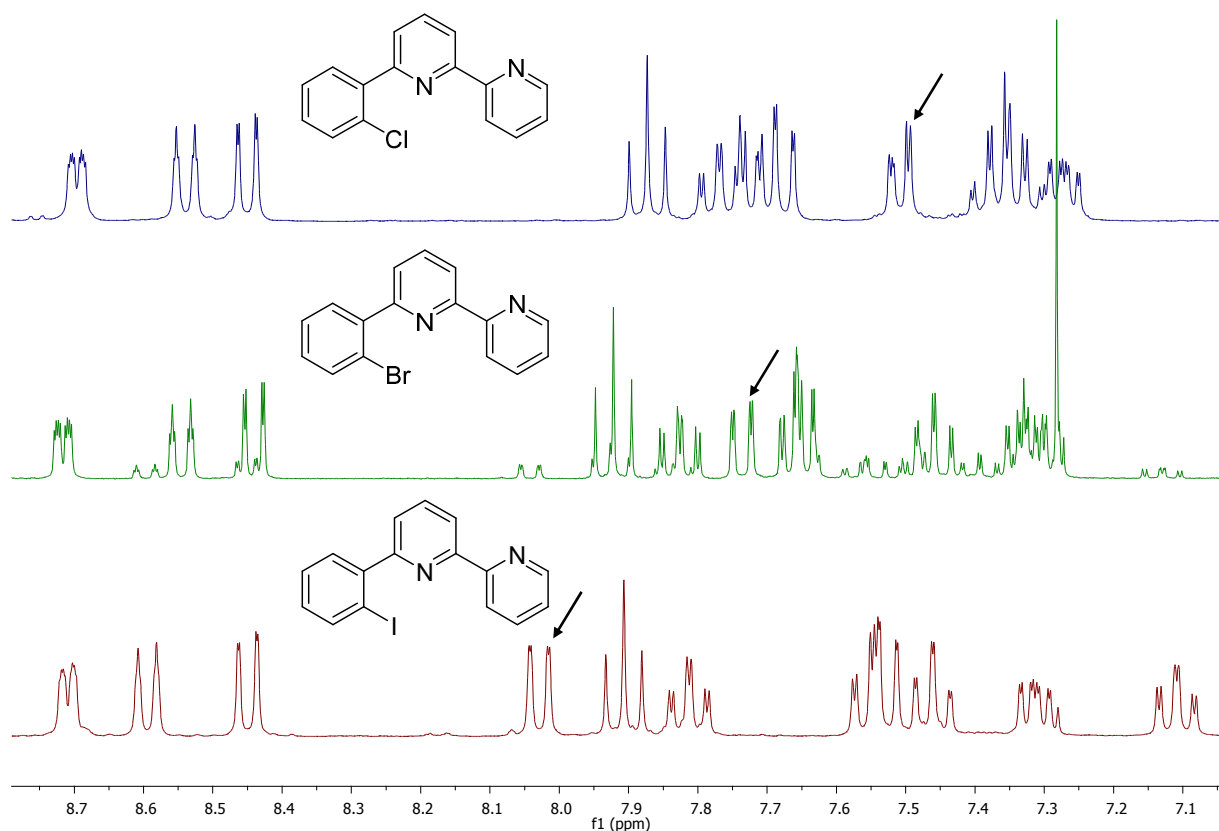


Figure S2. 300 MHz ^1H NMR spectra of the protoligands X-Phbpy in CDCl_3 . Arrows mark the signals for $\text{H}_{3'}$ which is increasingly de-shielded through the X atom along the series $\text{Cl} < \text{Br} < \text{I}$.

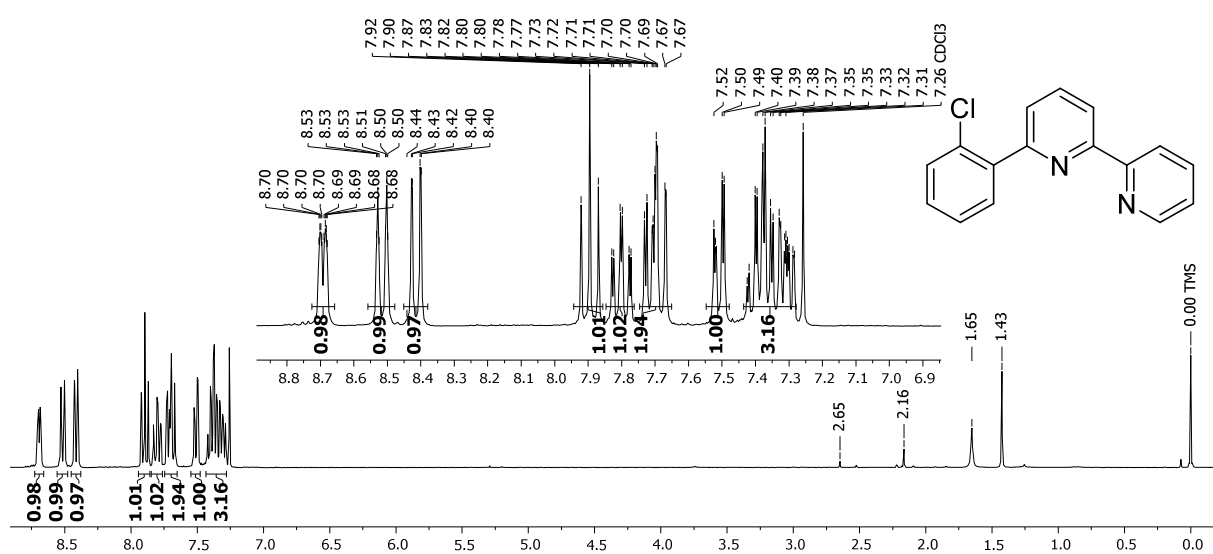


Figure S3. 300 MHz ^1H NMR spectrum of Cl-Phbpy in CDCl_3 .

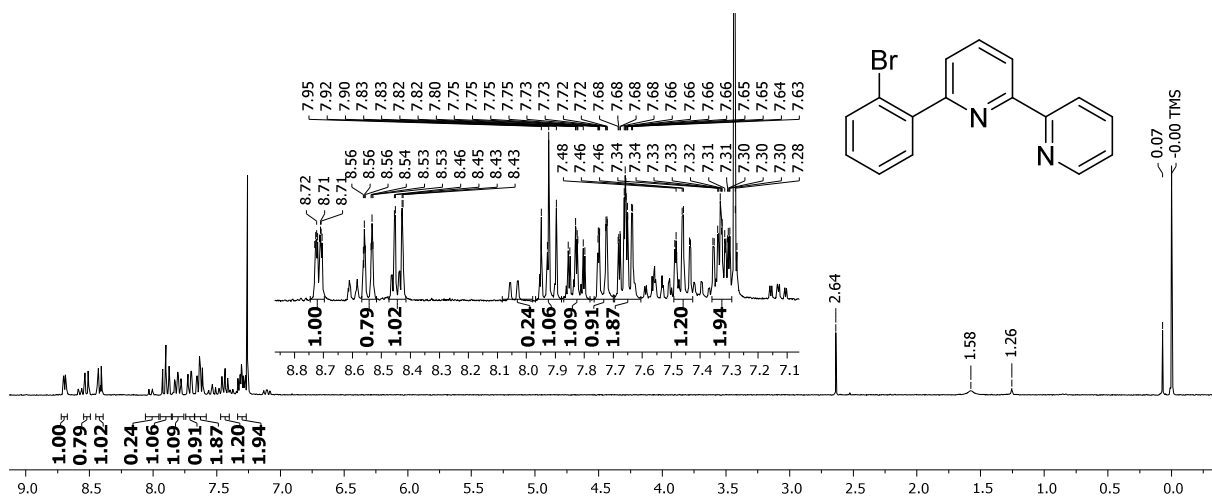


Figure S4. 300 MHz ¹H NMR spectrum of Br-Phbpy in CDCl₃.

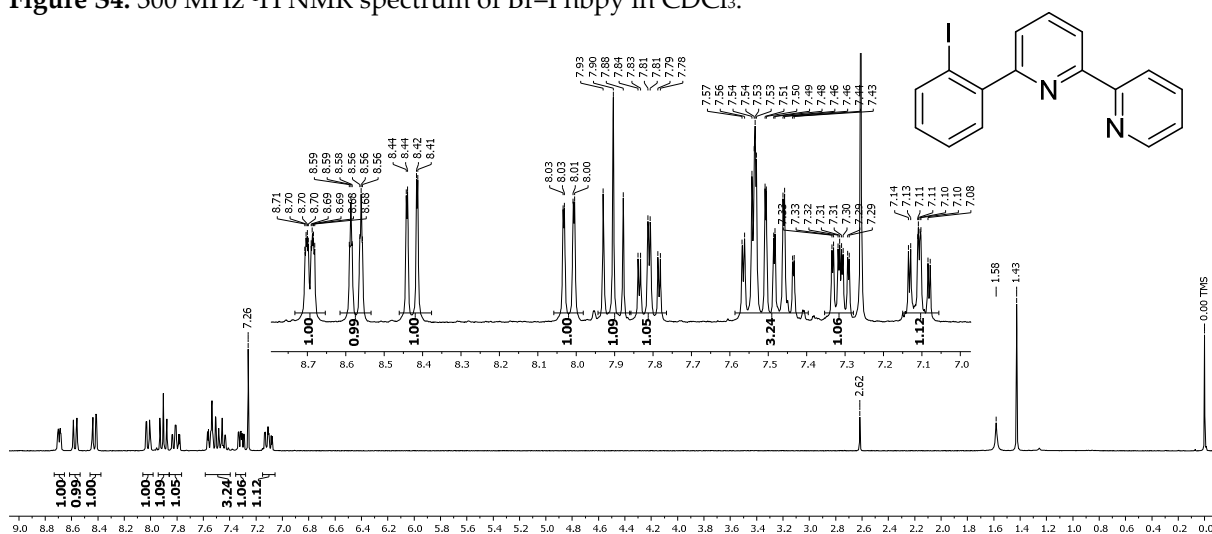


Figure S5. 300 MHz ¹H NMR spectrum of I-Phbpy in CDCl₃.

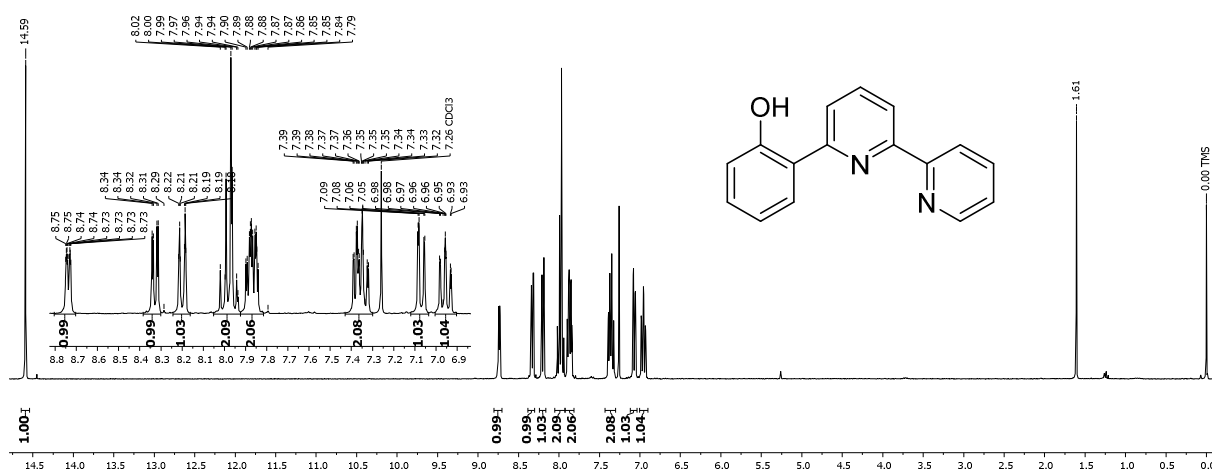


Figure S6. 300 MHz ¹H NMR spectrum of HO-Phbpy in CDCl₃.

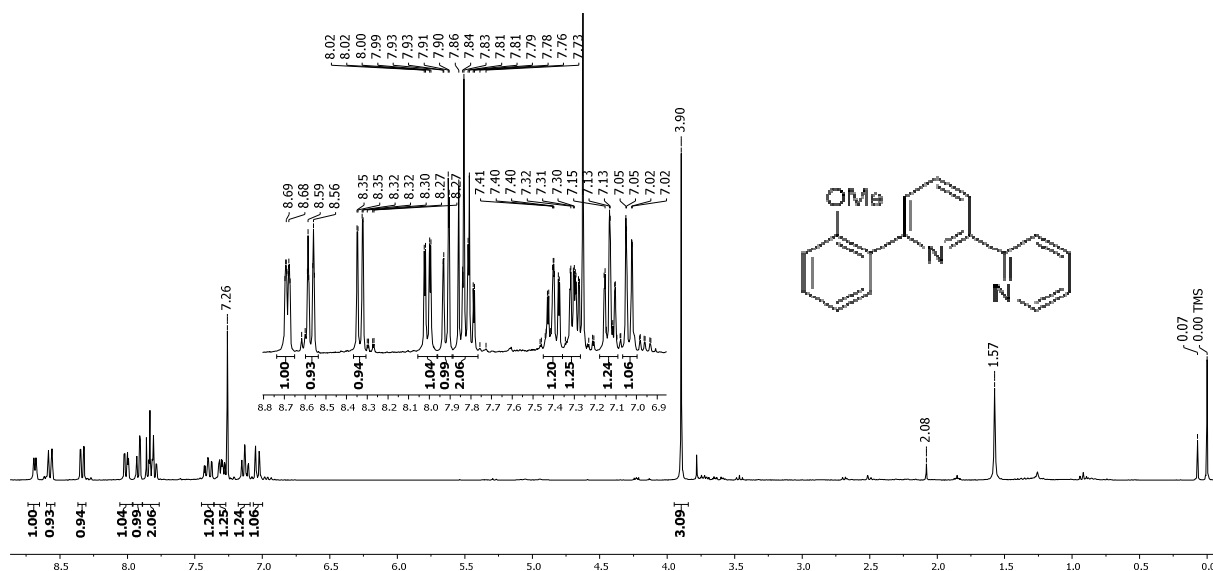


Figure S7. 300 MHz ^1H NMR spectrum of MeO-Phbpy in CDCl_3 .

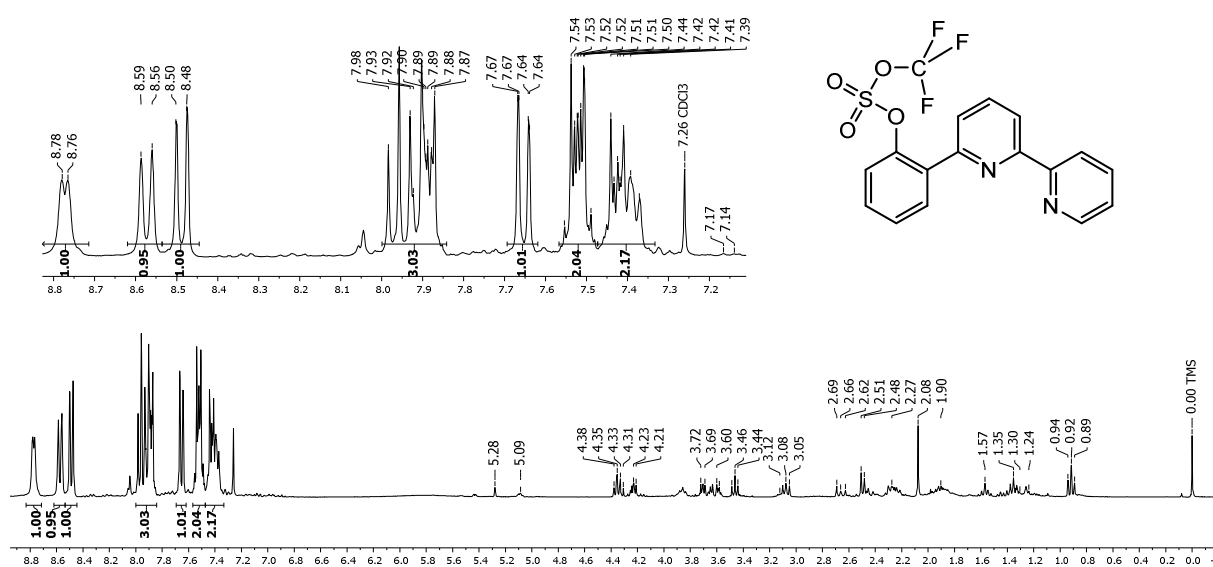


Figure S8. 300 MHz ^1H NMR spectrum of TfO-Phbpy in CDCl_3 .

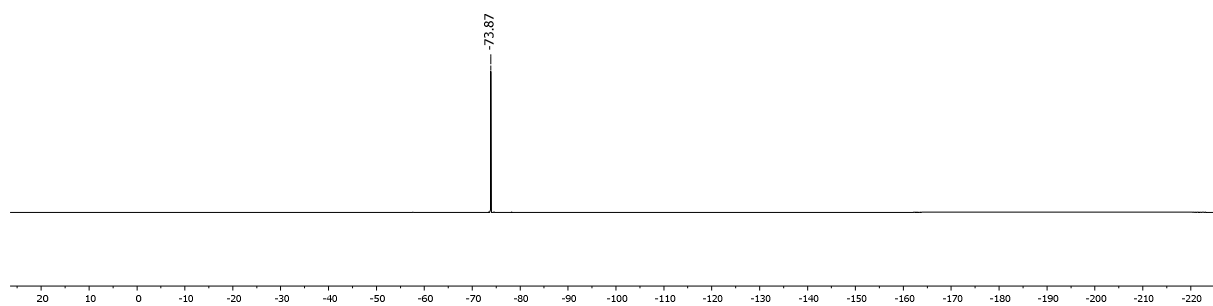


Figure S9. 282 MHz ^{19}F NMR spectrum of TfO-Phbpy in CDCl_3 .

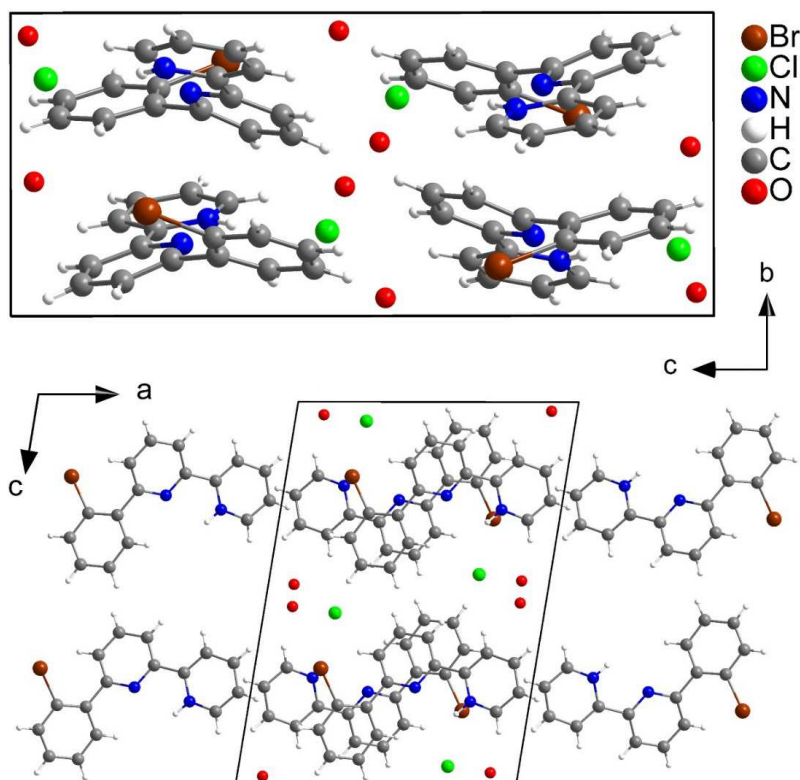


Figure S10. Views on the crystal structure of [BrPhbpyH]Cl·2H₂O along the *a* (top) and *b* axes (bottom).

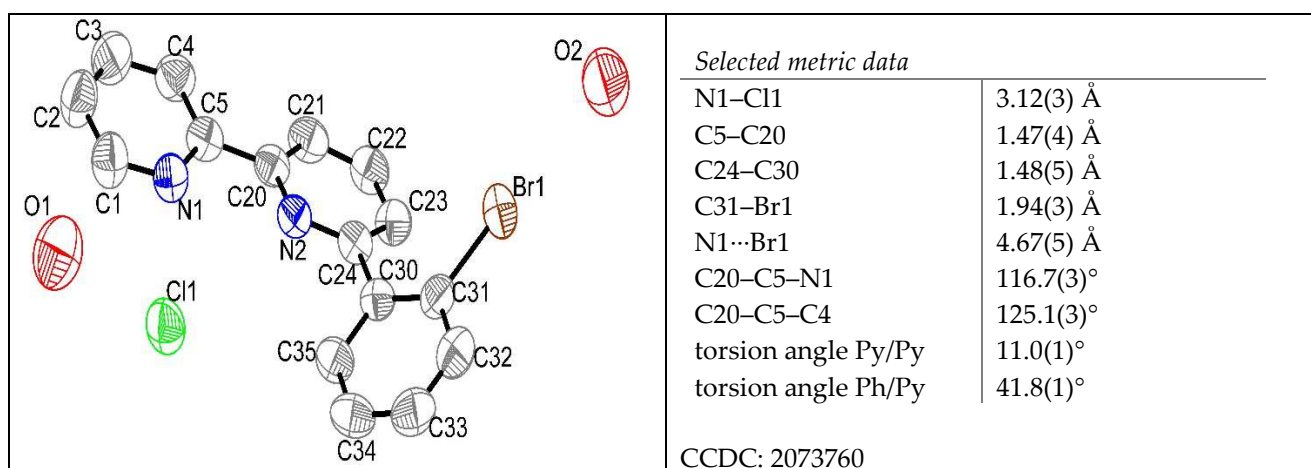


Figure S11. Molecular structure of [BrPhbpyH]Cl·2H₂O at 50% ellipsoid representation (left) and essential metric data (right).

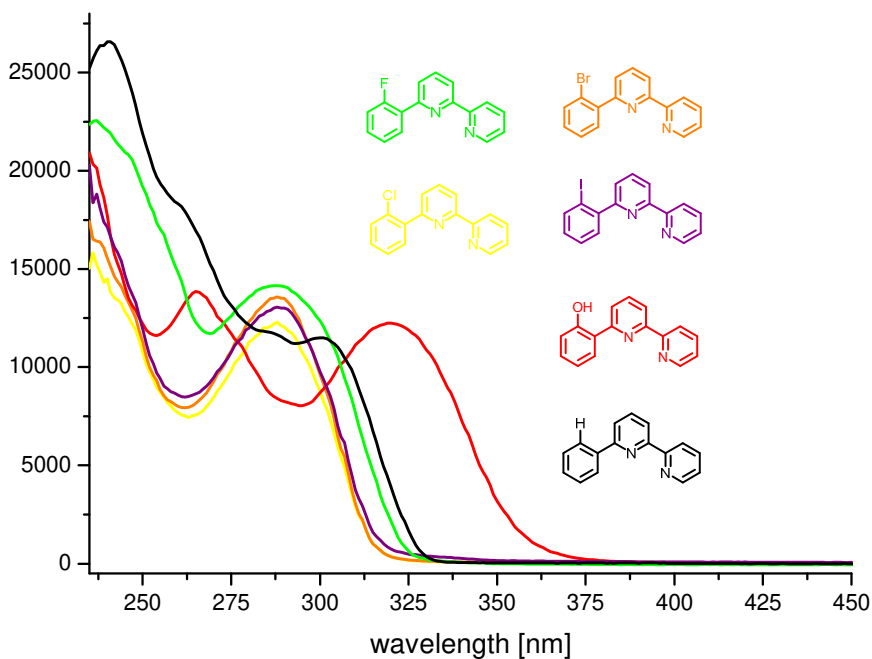


Figure S12. UV-vis absorption spectra of FPhbpv, ClPhbpv, BrPhbpv, IPhbpv, HOPhbpv, and HPhbpv in CH_2Cl_2 .

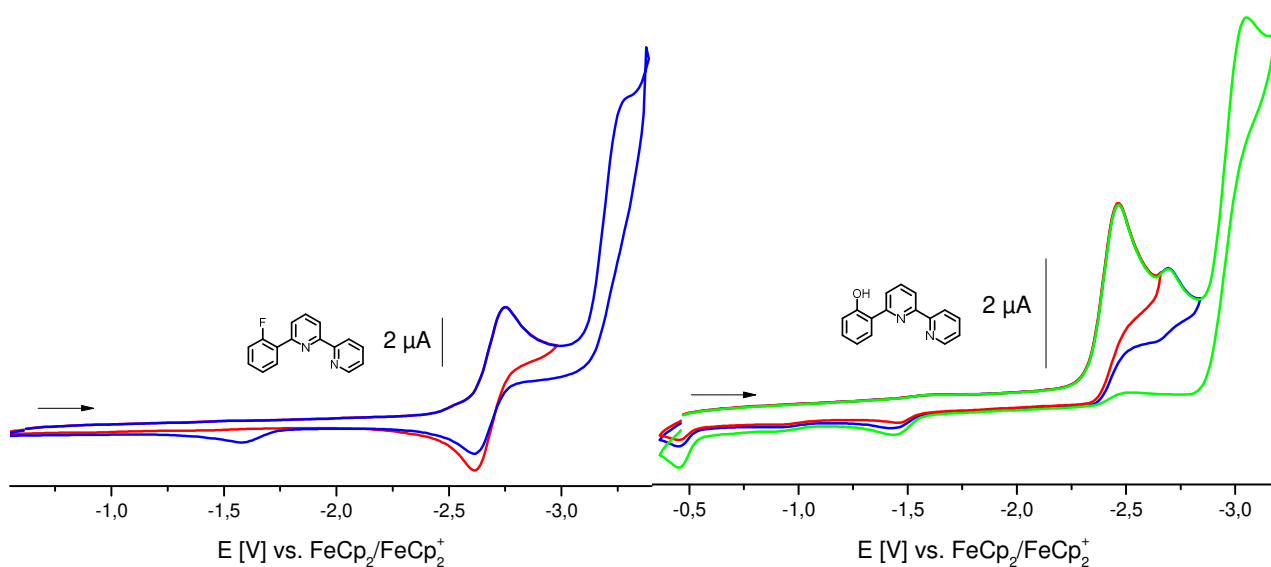


Figure S13. Cyclic voltammograms of FPhbpv (left) and HOPhbpv (right) in 0.1 M $n\text{-Bu}_4\text{NPF}_6/\text{THF}$ at 298 K and 0.1 V/s scan rate.

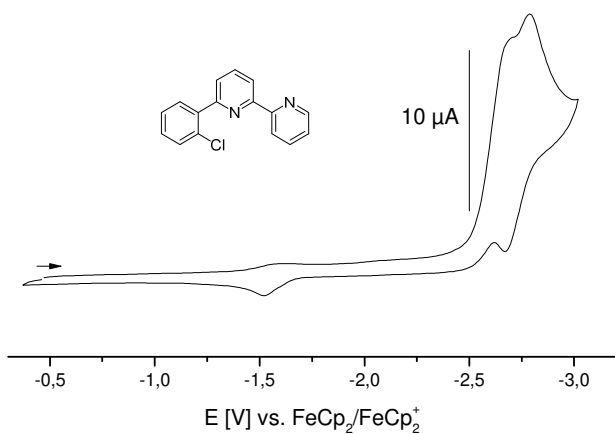


Figure S14. Cyclic voltammograms of ClPhbpv in 0.1 M $n\text{-Bu}_4\text{NPF}_6/\text{THF}$ at 298 K and 0.1 V/s scan rate.

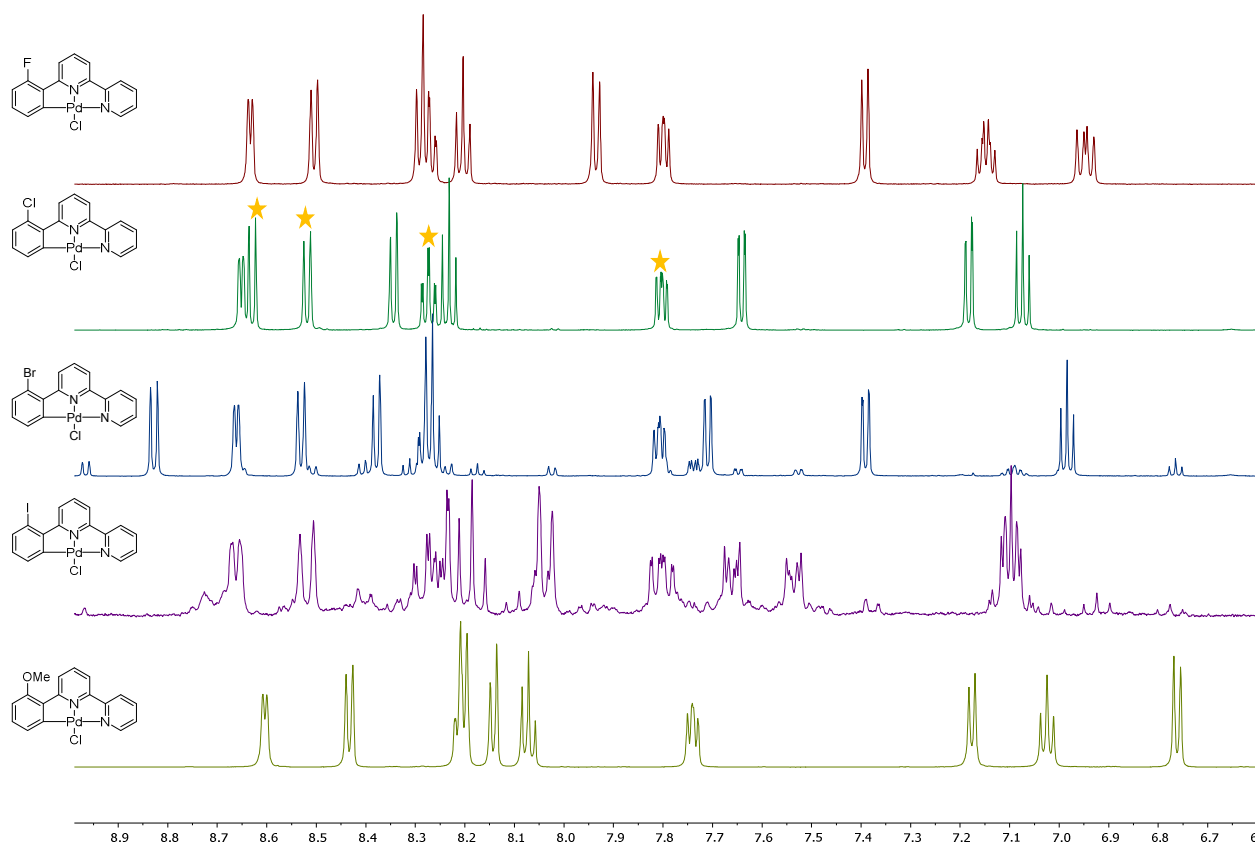


Figure S15. 600 MHz ^1H NMR spectra of $[\text{Pd}(\text{FPhbpy})\text{Cl}]$, $[\text{Pd}(\text{ClPhbpy})\text{Cl}]$, $[\text{Pd}(\text{BrPhbpy})\text{Cl}]$, $[\text{Pd}(\text{MeOPhbpy})\text{Cl}]$ and 300 MHz ^1H NMR of $[\text{Pd}(\text{IPhbpy})\text{Cl}]$ (from top to bottom) in DMSO-d_6 . Marked with an asterisk are signals of the peripheral pyridine moiety.

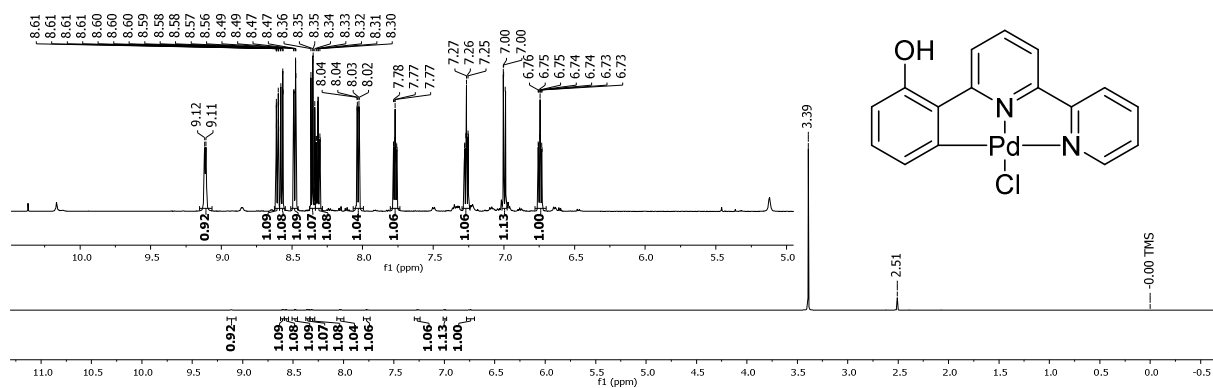


Figure S16. 600 MHz ^1H NMR spectrum of $[\text{Pd}(\text{OHPhbpy})\text{Cl}]$ in DMSO-d_6 .

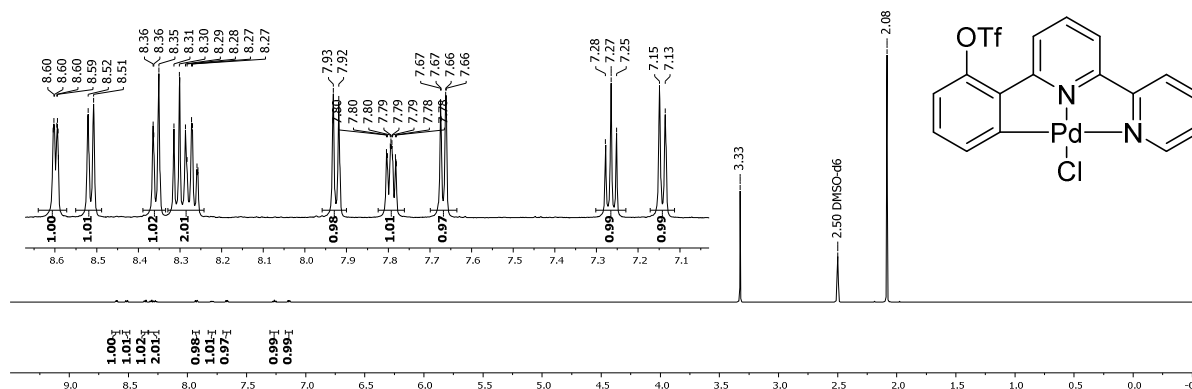


Figure S17. 600 MHz ^1H NMR spectrum of $[\text{Pd}(\text{TfOPhbpy})\text{Cl}]$ in DMSO-d_6 .

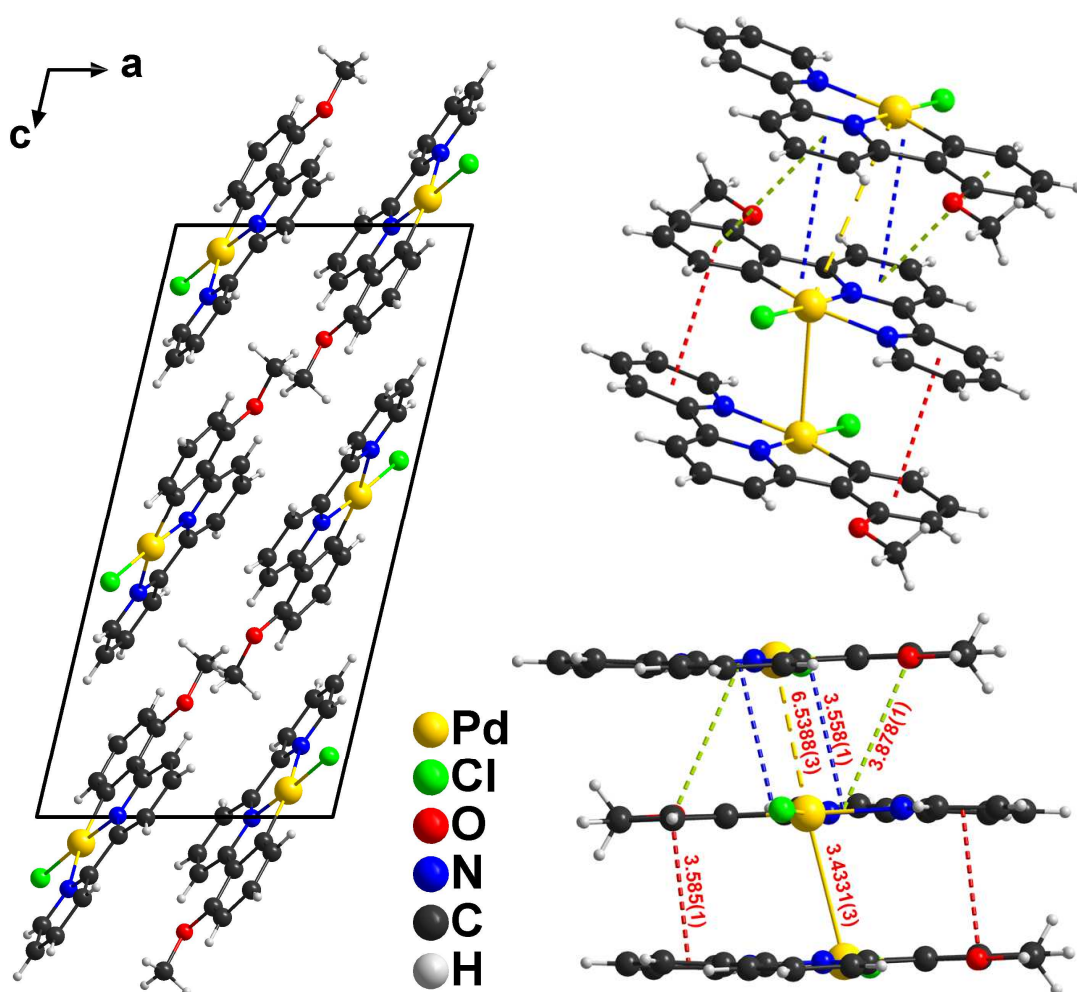


Figure S18. View on the Unit cell of [Pd(MeOPhppy)Cl] along the crystallographic *b* axis (left). Selected π stacking and Pd-Pd contacts (right). Colour code: blue(dashed): 3.558(1) Å; red(dashed): 3.585(1) Å; green(dashed): 3.878(1). Pd-Pd: yellow(dashed): 6.5388(3) Å; yellow(solid): 3.4331(3) Å.

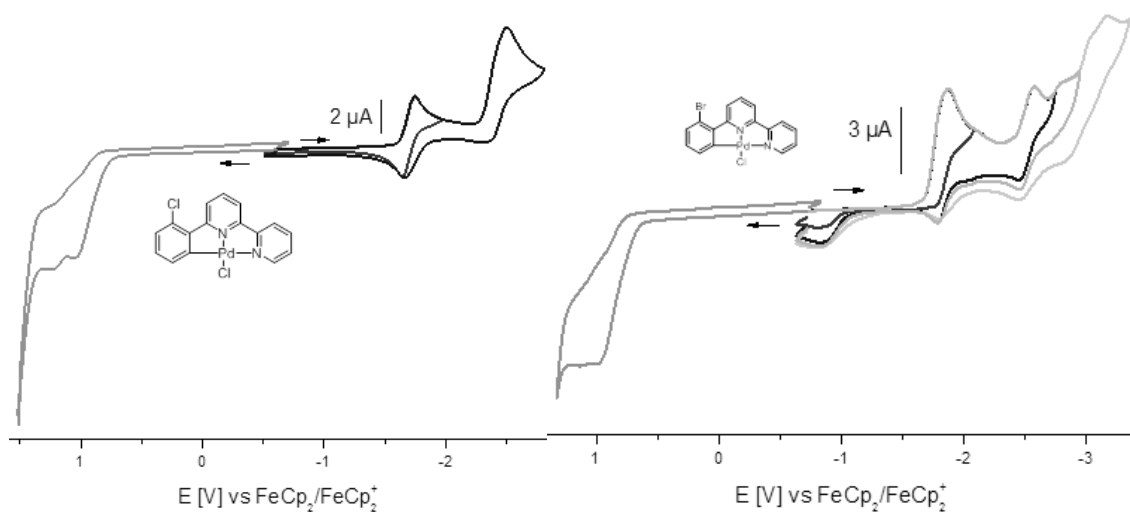


Figure S19. Cyclic voltammograms of [Pd(ClPhppy)Cl] (left) and [Pd(BrPhppy)Cl] (right) in 0.1 M *n*-Bu₄NPF₆/THF at 298 K and 0.1 V/s scan rate.

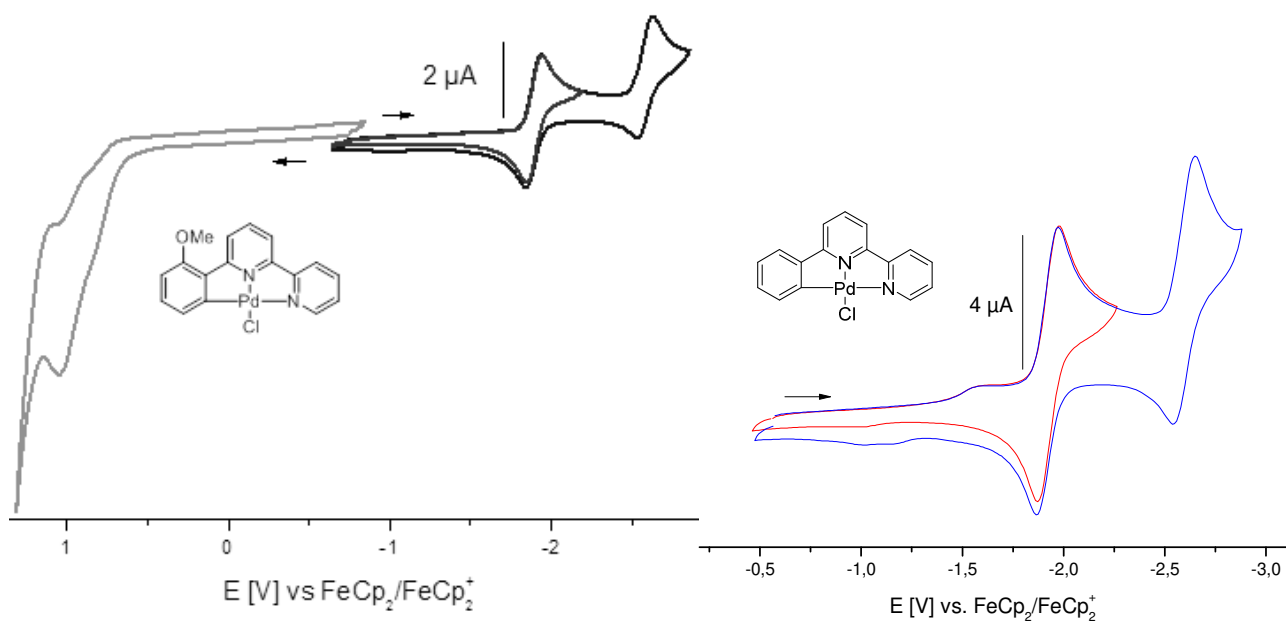


Figure S20. Cyclic voltammograms of $[\text{Pd}(\text{MeOPhbpv})\text{Cl}]$ (left) and $[\text{Pd}(\text{Phbpv})\text{Cl}]$ (right) in $0.1 \text{ M } n\text{-Bu}_4\text{NPF}_6/\text{THF}$ at 298 K and 0.1 V/s scan rate.

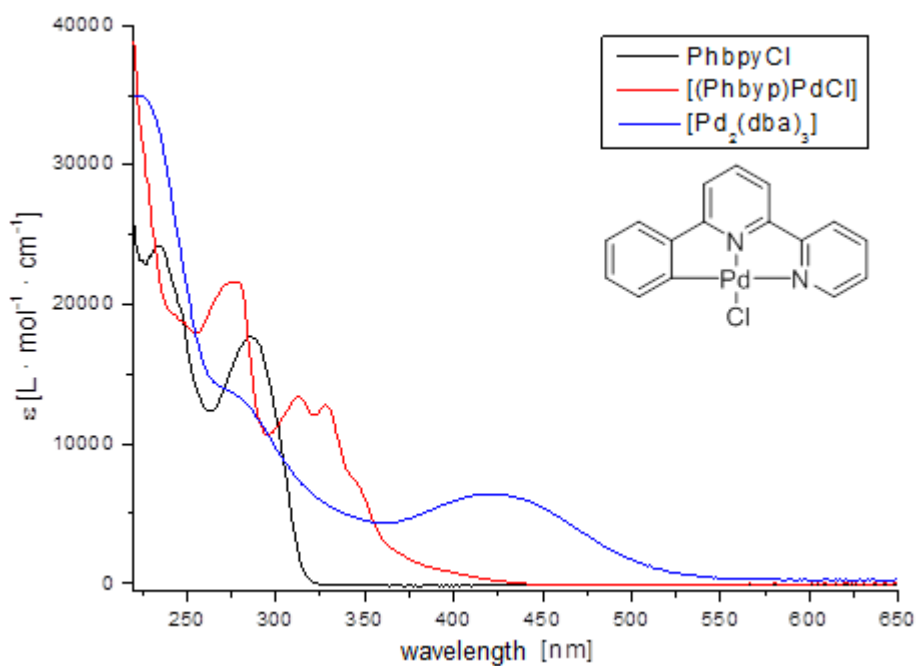


Figure S21. UV-vis absorption spectra of ClPhbpv (black trace), $[\text{Pd}_2(\text{dba})_3]$ (blue trace), and $[\text{Pd}(\text{Phbpv})\text{Cl}]$ (red trace) in THF.

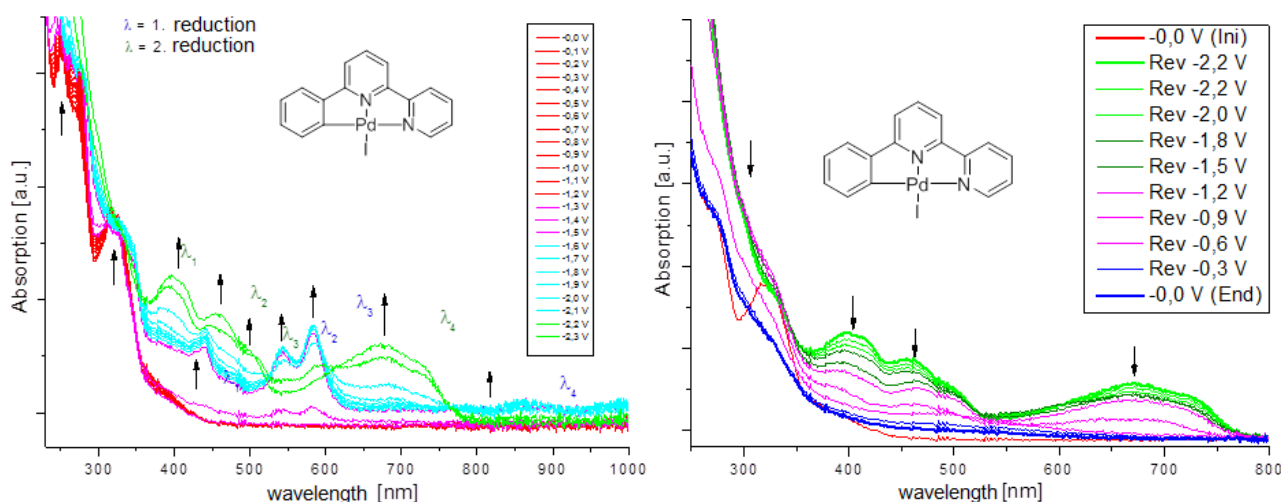


Figure S22. UV-vis absorption spectra of [Pd(Phbpy)I] during electrochemical reduction (left) and re-oxidation (right) in 0.1 M *n*-Bu₄NPF₆/THF.

Supplementary Tables

Table S1. UV-vis absorption maxima of the protoligands X/Y-Phbpy. ^a

	λ_1 (ϵ)	λ_2 (ϵ)	λ_3 (ϵ)	λ_4 (ϵ)	λ_5 (ϵ)	λ_6 (ϵ)
HPhbpy	-	241 (26.6)	-	260 (18.3)	286 (11.9)	300 (11.5)
FPhbpy	237 (22.6)	-	246 (20.9)	256 (16.8)	287 (14.2)	-
ClPhbpy	-	243 (13.6)	248 (12.1)	-	288 (12.2)	-
BrPhbpy	238 (16.4)	243 (14.2)	-	254 (9.4)	288 (13.6)	307 (5.6)
IPhbpy	240 (17.2)	243 (16.0)	246 (13.0)	255 (10.5)	288 (13.0)	-
HOPhbpy	237 (20.2)	243 (15.6)	247 (13.2)	265 (13.8)	278 (11.2)	320 (12.3)

^a Measured in CH₂Cl₂; λ = absorption maximum in nm, ϵ = molar extinction coefficient in 1000 L·mol⁻¹·cm⁻¹.

Table S2. Crystal structure and refinement data of [BrPhbpyH]Cl·2H₂O.

Formula	C ₁₆ H ₁₆ N ₂ BrClO ₂
Molar weight	382.01 g·mol ⁻¹
Crystal system,	monoclinic
Space group	<i>P</i> 2 ₁ / <i>c</i>
Cell	<i>a</i> = 12.73(8) Å, <i>b</i> = 7.45(3) Å, β = 99.3(5)° <i>c</i> = 17.65(1) Å, <i>V</i> = 1654.3 Å ³
Volume	<i>V</i> = 1654.3 Å ³
Formula units <i>Z</i>	4
Calculated density	1.524 g·cm ⁻³
F(000)	760
Collected / independent reflections	24088 / 3512
<i>R</i> _{int}	0.0778
Final <i>R</i> values (<i>I</i> > 2σ(<i>I</i>))	<i>R</i> ₁ = 0.0437, w <i>R</i> ₂ = 0.1162
<i>R</i> values all data	<i>R</i> ₁ = 0.0739, w <i>R</i> ₂ = 0.1322
Goodness of fit on <i>F</i> ²	1.019
Residual electrons and holes	0.456 / -0.3000 e·Å ⁻³
CCDC	2073760

Table S3. Selected structural parameters of [Pd(MeOPhppy)Cl] and [Pd(FPhppy)Cl].^a

	[Pd(MeOPhppy)Cl]	[Pd(FPhppy)Cl]	[Pd(Phppy)Cl] [2] ^b
Distances / Å			
Pd(1)–C(22)	1.979(2)	1.9897(5)	2.067(3) ^b
Pd(1)–N(2)	2.1382(2)	2.1304(4)	2.067(3) ^b
Pd(1)–N(1)	1.9531(2)	1.9306(4)	1.960(4)
Pd(1)–Cl(1)	2.3216(5)	2.2806(2)	2.317(1)
C(26)–O(1)	1.370(3)	1.3316(7) (C(26)–F(1))	-
N(2)–C(22)	4.0622(3)	4.0658(6)	4.04(1)
C1–C21	1.461(3)	1.458(6)	1.455(4) ^b
C5–C11	1.478(3)	1.481(7)	1.455(4) ^b
C26–X	(OMe)1.370(3)	(F)1.332(7)	(H)0.960(4)
Angles / °			
C(22)–Pd(1)–N(1)	81.82(8)	81.731(2)	80.3(1) ^b
N(1)–Pd(1)–N(2)	79.43(7)	79.655(2)	80.3(1) ^b
N(2)–Pd(1)–Cl(1)	100.42(5)	99.791(1)	99.7(1) ^b
Cl(1)–Pd(1)–C(22)	98.27(6)	98.832(1)	99.7(1) ^b
N(1)–(Pd1)–(Cl1)	177.43(5)	179.027(1)	180.0(1)
N(2)–(Pd1)–(C22)	161.22(8)	161.365(2)	159.9(1)
C26–C21–C1–C2	2.3(3)	0.1(9)	0.1(5) ^b
C4–C5–C11–C12	6.3(3)	4.3(9)	0.1(5) ^b
C24–C23–C22–Pd	0.2(2)	0.2(5)	0.5(3) ^b
C14–C15–N2–Pd	4.0(2)	4.3(5)	0.5(3) ^b
C4–C5–N1–Pd	3.4(2)	1.2(4)	0.1(2) ^b
C2–C1–N1–Pd	3.4(1)	0.2(4)	0.1(2) ^b
Σ angles around Pd	359.94	360.0	360

^a Crystal structure and refinement data in Table 1 in the manuscript. ^b Pairwise identical values due to C₂-symmetry (space group C2/c) of the molecule, from Ref. [2].

Table S4. UV-vis absorption maxima Pd complexes [Pd(XPhppy)X]^a

	λ ₁ (ε)	λ ₂ (ε)	λ ₃ (ε)	λ ₄ (ε)	λ ₅ (ε)	λ ₆ (ε)
[Pd(Phppy)Cl]	266 (20) sh	278 (21)	311 (12)	325 (13)	342 (8) sh	402 (1) sh
[Pd(Phppy)Br]	266 (21) sh	281 (20)	314 (15)	329 (14)	345 (8) sh	402 (1) sh
[Pd(Phppy)I]	249 (30)	269 (22)	319 (15)	330 (14) sh	345 (9) sh	395 (3) sh
[Pd(FPhppy)Cl]	264 (20)	279 (26)	310 (12)	325 (12)	338 (10) sh	402 (1) sh
[Pd(ClPhppy)Cl]	264 (19)	282 (17)	311 (11)	327 (11)	343 (8) sh	402 (1) sh
[Pd(BrPhppy)Cl]	265 (21)	282 (17)	311 (12)	328 (12)	344 (9) sh	402 (1) sh
[Pd(TfOPhppy)Cl]	262 (20)	277 (20)	306 (14)	321 (13)	334 (9)	402 (1) sh
[Pd(MeOPhppy)Cl]	268 (13)	284 (12)	312 (8)	327 (7) sh	353 (5) sh	418 (1) sh
[Pd(HOPhppy)Cl]	248 (27)	290 (10) sh	323 (7)	340 (7)	394 (5)	448 (3) sh
[Ni(Phppy)Cl] ^b	281		321	354	391	596
[Pt(Phppy)Cl] ^b	278	302	330	363	410	430

^a Measured in CH₂Cl₂; λ = absorption maximum in nm, ε = molar extinction coefficient in 1000 L·mol⁻¹·cm⁻¹.

Table S5. Selected TD-DFT-calculated long-wavelength singlet transitions and UV-vis absorption maxima of [Pd(Phppy)Cl]^a

Absorption / nm	Starting orbital	Target orbital	Contribution / %
402	HOMO	LUMO	83
395	HOMO-2	LUMO	77
368	HOMO	LUMO+1	45
	HOMO-4	LUMO	36
	HOMO-2	LUMO+1	28

	HOMO-3	LUMO+1	49
361	HOMO-2	LUMO+1	13
	HOMO-4	LUMO	16
	HOMO-2	LUMO+1	27
	HOMO-3	LUMO+1	22
	HOMO-4	LUMO	18

^a Calculations were performed on B3LYP level using the basis sets def2-TZV(P) for C, H, N, O and LAN-L2DZ for Pd (ECP: Hay/Wadt (n-1)) [3-5]. The percentages represent the contribution of the described transition in the excitation process.

Table S6. Selected TD-DFT-calculated long-wavelength singlet transitions and UV-vis absorption maxima of [Pd(ClPhbpy)Cl]^a

Absorption / nm	Starting orbital	Target orbital	Contribution / %
477	HOMO	LUMO	89
443	HOMO-2	LUMO	83
387	HOMO	LUMO+1	85
366	HOMO-4	LUMO	66
	HOMO-2	LUMO+1	20
363	HOMO-3	LUMO+1	59
	HOMO-2	LUMO+1	17
	HOMO-4	LUMO	11
361	HOMO-2	LUMO+1	37
	HOMO-3	LUMO+1	30
	HOMO-4	LUMO	14

^a Only maxima with $\lambda > 350$ nm and oscillator strength above 0.01. Calculations were performed on B3LYP level using the basis sets def2-TZV(P) for C, H, N, O and LAN-L2DZ for Pd (ECP: Hay/Wadt (n-1)) [3-5]. The percentages represent the contribution of the described transition in the excitation process.

Table S7. Selected DFT-calculated long-wavelength transitions and UV-vis absorption maxima of [Pd(OHPhbpy)Cl]^a

Absorption / nm	Starting orbital	Target orbital	Contribution / %
singlet			
474	HOMO	LUMO	93
443	HOMO-2	LUMO	84
triplet			
441	HOMO-4	LUMO	62
	HOMO-2	LUMO	21
singlet			
399	HOMO-4	LUMO	87
381	HOMO	LUMO+1	86
362	HOMO-2	LUMO+1	76
triplet			
422	HOMO-4	LUMO+1	43
	HOMO	LUMO+1	23
406	HOMO	LUMO+1	47
	HOMO-2	LUMO+1	29
singlet			
286	HOMO-7	LUMO	35
	HOMO-6	LUMO	32
	HOMO-4	LUMO+2	16

^a Calculations were performed on B3LYP level using the basis sets def2-TZV(P) for C, H, N, O and LAN-L2DZ for Pd (ECP: Hay/Wadt (n-1)) [3-5]. The percentages represent the contribution of the described transition in the excitation process.

Table S8. Selected TD-DFT-calculated long-wavelength singlet transitions and UV-vis absorption maxima of [Pd(MeOPhbpv)Cl]^a

Absorption / nm	Starting orbital	Target orbital	Contribution / %
475	HOMO	LUMO	92
446	HOMO-2	LUMO	80
410	HOMO-3	LUMO	85
	HOMO-2	LUMO	11
382	HOMO	LUMO+1	87
363	HOMO-2	LUMO+1	77

^a Only maxima with $\lambda > 350$ nm and oscillator strength above 0.01. Calculations were performed on B3LYP level using the basis sets def2-TZV(P) for C, H, N, O and LAN-L2DZ for Pd (ECP: Hay/Wadt (n-1)) [3-5]. The percentages represent the contribution of the described transition in the excitation process.

References

- (1) E. A. Krasnokutskaya, N. I. Semenischeva, V. D. Filimonov, P. Knochel, A new, One-Step, Effective Protocol for the Iodination of Aromatic and Heterocyclic Compounds via Aprotic Diazotization of Amines, *Synthesis* **2006**, 1, 81-84
- (2) Constable, E. C.; Henney, R. P. G.; Leese, T. A.; Tocher, D. A. Cyclopalladated and Cycloplatinated Complexes of 6-Phenyl-2,2'-bipyridine: Platinum-Platinum Interactions in the Solid State. *J. Chem. Soc., Chem. Commun.* **1990**, 513–515.
- (3) P. J. Hay, W. R. Wadt, "Ab initio effective core potentials for molecular calculations – potentials for the transition-metal atoms Sc to Hg," *J. Chem. Phys.*, **1985**, 82, 270–283.
- (4) P. J. Hay, W. R. Wadt, Ab initio effective core potentials for molecular calculations – potentials for K to Au including the outermost core orbitals, *J. Chem. Phys.*, **1985**, 82, 299–310.
- (5) L. E. Roy, P. J. Hay, R. L. Martin, Revised Basis Sets for the LANL Effective Core Potentials, *J. Chem. Theory Comput.* **2008**, 4, 1029–1031.